

## Article

# Hydrodynamic Model Ensembles for Climate Change Projections in Estuarine Regions

Isabel Iglesias <sup>1,\*</sup>, Ana Bio <sup>1</sup>, Willian Melo <sup>2</sup>, Paulo Avilez-Valente <sup>1,3</sup>, José Pinho <sup>2</sup>, Mariana Cruz <sup>4</sup>, Ana Gomes <sup>2</sup>, José Vieira <sup>2</sup>, Luísa Bastos <sup>1,5</sup> and Fernando Veloso-Gomes <sup>1,3</sup>

<sup>1</sup> Interdisciplinary Centre of Marine and Environmental Research (CIIMAR/CIMAR), University of Porto, 4450-208 Matosinhos, Portugal; anabio@ciimar.up.pt (A.B.); pvalente@fe.up.pt (P.A.-V.); lcbastos@fc.up.pt (L.B.); vgomes@fe.up.pt (F.V.-G.)

<sup>2</sup> Centre of Territory, Environment and Construction (CTAC), Department of Civil Engineering, University of Minho, 4800-058 Guimarães, Portugal; willianwm94@gmail.com (W.M.); jpinho@civil.uminho.pt (J.P.); carolina\_gomes@live.com (A.G.); jvieira@civil.uminho.pt (J.V.)

<sup>3</sup> Faculty of Engineering, University of Porto, 4200-465 Porto, Portugal

<sup>4</sup> Faculty of Sciences, University of Minho, 4704-553 Braga, Portugal; marianarmcruz@gmail.com

<sup>5</sup> Department of Geosciences Environment and Spatial Planning, Faculty of Sciences, University of Porto, 4169-007 Porto, Portugal

\* Correspondence: iglesias@ciimar.up.pt; Tel.: +351-223-401-800

**Abstract:** In the current context of climate change, understanding the effects of the changing conditions on estuaries is of utmost importance to protect populations and ecosystems. Given the diversity of impacts depending on the region, there is a need for local and dedicated studies to understand and mitigate the risks. Numerical models can provide forecasts of extreme floods and sea-level rise (SLR). However, they can present inaccuracies. In this work, the ensemble technique was applied to improve the numerical modeling forecasting for estuaries by considering scenarios of extreme river flow discharges (EFDs) and SLR scenarios for 2050 and 2100. The simulations were performed for two different estuarine regions in northern Portugal, and the superensemble was constructed with the results of two different numerical models. The results differed per estuary, highlighting the importance of a local approach. For the Douro estuary dynamics, the results showed that for the EFD, the effects of the SLR were not noticeable, indicating that, in this estuary, the river component was more important than the maritime component. In contrast, the Minho estuary dynamics were found to be affected by the SLR along the whole estuarine region, indicating a maritime influence and a worsening of the flood conditions for future scenarios.

**Keywords:** estuaries; hydrodynamics; ensemble; numerical models; extreme events; climate change



**Citation:** Iglesias, I.; Bio, A.; Melo, W.; Avilez-Valente, P.; Pinho, J.; Cruz, M.; Gomes, A.; Vieira, J.; Bastos, L.; Veloso-Gomes, F. Hydrodynamic Model Ensembles for Climate Change Projections in Estuarine Regions. *Water* **2022**, *14*, 1966. <https://doi.org/10.3390/w14121966>

Academic Editor: Jin Teng

Received: 18 May 2022

Accepted: 15 June 2022

Published: 20 June 2022

**Publisher's Note:** MDPI stays neutral with regard to jurisdictional claims in published maps and institutional affiliations.



**Copyright:** © 2022 by the authors. Licensee MDPI, Basel, Switzerland. This article is an open access article distributed under the terms and conditions of the Creative Commons Attribution (CC BY) license (<https://creativecommons.org/licenses/by/4.0/>).

## 1. Introduction

Estuarine regions are important from an ecological, economic, and social point of view. They are highly variable transition zones that link land, freshwater, and marine environments. Therefore, they are densely populated, concentrating human settlements, leisure activities, fisheries, and other marine industries that exploit their natural resources. At the same time, they process nutrients and pollutants, playing a key role in the cycling of carbon and other biogenic elements, and providing shelter and nursery areas for many species. Estuaries are highly productive areas, essential not only for fisheries and nature conservation but also as natural protection against floods and storms. Changes in their configuration can thus have high socio-economic costs [1,2].

In the last few decades, the population, economic assets, and urbanization in estuarine regions have experienced rapid growth, and a continuous increase in population is expected for the near future [3,4]. The intensification of man-made interventions and anthropogenic activities in estuaries enhances their vulnerability. Moreover, in the present context of

climate change, environmental conditions in estuaries can be even more challenging. The complex estuarine systems can be considered one of the most sensitive areas to environmental stressors due to the strong coupling between physics, sediments, chemistry, and biology [5,6]. In this sense, the effects of the climate change conditions in estuaries can be diverse, resulting in changes in river flow, extreme events frequency, and changes in water temperature and water level, affecting the circulation, salinity distribution, suspended sediments, dissolved oxygen, and biogeochemistry [7].

Changes in river flow will produce alterations in the circulation, the mixing of the water masses, and the sedimentation patterns, as well as in nutrient delivery, primary production, the residence time of the water masses, and the environmental conditions [1]. An increase in river flows can alter the estuarine configuration from well mixed to partially mixed or to highly stratified estuaries. Furthermore, flood discharges can remobilize large quantities of stored sediments [6]. Considering that an increase in the frequency and strength of extreme events was reported [4], marked changes in future estuarine dynamics are expected, which may unbalance morphodynamic patterns and impact tidal propagation and estuarine circulation in general. In contrast, a decrease in river flows can increase the average salinity. Given that the estuarine biota is highly sensitive to salt intrusion, problems in the reproductive success of this biota are expected, with a reduction in the primary production and fisheries. At the same time, subtidal species can penetrate deeper into estuaries, occupying the space of other native species [8].

Another expected change is the warming of estuarine waters. This warming will decrease the surface water density and promote stratification. At the same time, this warming can intensify microbial pathogen concentrations, increasing public health risks [8]. However, the effects of the salinity outweigh those of temperature in the main water body [6]. The effect of the sea level rise will cause an increased salt-wedge penetration in the estuary and the retention of sediments in the lower river courses. It will also affect the response of the estuary to extreme flow and wave conditions, increasing the probability of overtopping and floods. At the same time, changes in the sea level can produce changes in the tidal range, increasing the tidal velocities and, consequently, the vertical mixing, as well as sediment transport, thus deepening the estuary. A change in the tidal range or sea level may change the estuary from being a flood-dominant to an ebb-dominant system [6]. In terms of biogeochemistry, a sea-level rise can produce an expansion of some marine habitats, whereas others may wane [8].

All those potential effects on the fauna, flora, and human activities can increase the erosion and loss of land to the sea, resulting in the loss of property, habitats and ecosystems, augmenting damage to infrastructures, and even forcing population displacement; they can affect human wellbeing, cause injuries, and even cause loss of life [8–12]. In this context, scientific and technical information has to be made available to decision makers to reduce vulnerability, increase resilience, and implement proper mitigation measures that support sustainable management [2].

Numerical models were shown to be adequate tools to improve the knowledge of estuarine dynamics and to forecast the effects of anthropogenic activities, extreme events, and climate change conditions [13]. They can be used to assess the effect of each forcing driver, representing the impact of changes in initial and boundary conditions, topo-bathymetric features, and coastal structures [14,15]. They can help to overcome the lack of field observations, allowing for a full characterization of the hydrodynamic patterns of estuarine regions and providing valuable information to promote population, services, and ecosystem safety [16]. At the same time, the outcomes of the modeling systems for different scenarios can help to optimize water resources management and implement forecasting and warning systems. In several studies, numerical modeling tools were implemented for estuarine regions to represent the effect of climate change on estuarine hydrodynamics and circulation [17,18], salinity patterns [19], water quality [20], morphodynamic evolution [21], and water level elevation and storm surges [22–24], revealing the utility of these tools

in forecasting future states of estuarine regions and providing key information to apply adaptation strategies.

The available modeling tools allow for an almost complete and high-resolution representation of the physical conditions in estuarine areas. However, models are simplifications of the reality and every modeling system has its strengths and weaknesses. Modeling results will therefore present a wide variety of uncertainties related to errors, calibration parameters, and model assumptions, as well as the approximations used for the initial conditions and the forcing characteristics [16]. Furthermore, in the context of climate change, predictions will depend on an adequate definition of the future climate and weather [6]. Given the need for accurate forecasts, finding and implementing new solutions that avoid or mitigate errors is crucial. In this context, ensemble modeling is considered one of the best solutions because it can minimize the combined uncertainty in input data, model parameters, and model structure, improving the performance of the models [25–28]. An ensemble uses statistical methods to combine several numerical model simulations. The obtained results present a smaller bias and variance than the individual solutions, improving the accuracy, reliability, and consistency of the final prediction [29,30]. This is a widely applied technique in atmospheric, climatic, and hydrological sciences [4,26,27,29,30]. Previous application of this technique to estuarine regions by Iglesias et al. [28] revealed that an adequate ensemble effectively improves the forecasting results of the individual models, even for the scenarios that were more difficult to forecast by single models. However, the ensemble technique, successfully applied in estuarine hydrodynamics [25,28], has not been fully developed to forecast future hydrodynamic patterns in estuarine regions considering climate change scenarios [4]. The objective of this work was to address this issue and apply the ensemble technique previously developed and implemented by Iglesias et al. [28] to forecast future scenarios for two different estuarine regions under climate change conditions.

## 2. Geographical Settings

Two different estuarine areas were considered in this study: the Douro and Minho estuaries (Figure 1). Despite the fact that these estuaries are separated by a distance of less than 100 km and present similar seasonal flow regimes, their river flow average and peak discharges, as well as their morphology, bathymetry, banks configuration, extension, and level of urbanization, are completely different, which is reflected in distinct dynamics and environmental conditions [2,28]. Therefore, separate studies were carried out to represent the local effects of climate change conditions and extreme events.

The Douro River estuary is located on the western coast of the Iberian Peninsula, reaching the Atlantic Ocean through a highly dynamic narrow urban estuary. It presents torrential regimes that produce strong currents and recurrent severe floods that cause serious damage to the riverine populations and fluvial navigation problems [31,32]. There are two main hydrodynamic drivers in this estuary: the freshwater flow and the tide. The freshwater flow is very dependent on the annual precipitation cycle (stronger during winter, weak during summer), but also on the hydropower production at the upstream dams that influence the water discharge schedule of the Crestuma–Lever dam. This last dam limits the estuarine extension to 21 km. The local tides have a semi-diurnal regime with a 12.4 h long period. Inside the estuary, tides are slightly progressive, with a small time delay from the mouth to the upstream end of the estuary and a small amplification [33]. During river floods, the freshwater masses are thoroughly flushed to the sea, inducing strong currents and preventing seawater intrusion, even in spring-tide conditions. For low river discharges, tidal currents become dominant, and the ocean water enters the estuary with a salt-wedge configuration [34]. The circulation patterns in the Douro estuary are also conditioned by the irregular bathymetry and the banks' configurations (Figure 1). Depths vary between 0 m and 10 m, although, depths up to 28 m can be found in narrower sections, outer bends, and sediment extraction sites [32]. At the southern margin of the estuary's mouth lies a wetland (São Paio Bay) and an estuarine sand spit made up of maritime and fluvial sediments. This sand spit partially obstructs the entry of ocean water, acting as a natural barrier against

storm waves and protecting the estuarine margins and harbors. To stabilize the sand spit, a seaward-facing detached breakwater was built, and the northern breakwater was extended (about 15 years ago). These structures interfere with local sedimentary and hydrodynamic patterns, significantly increasing the area and volume of the sand spit and silting up the contiguous wetland [31]. With its present configuration, it is likely that the sand spit will not be overtopped or rupture during extreme events (as it did before breakwater construction) such that future floods can be expected to cause severe economic losses and structural damage [16]. This becomes particularly relevant in the context of the predicted climate change effects, suggesting more severe extreme climate and flood events.

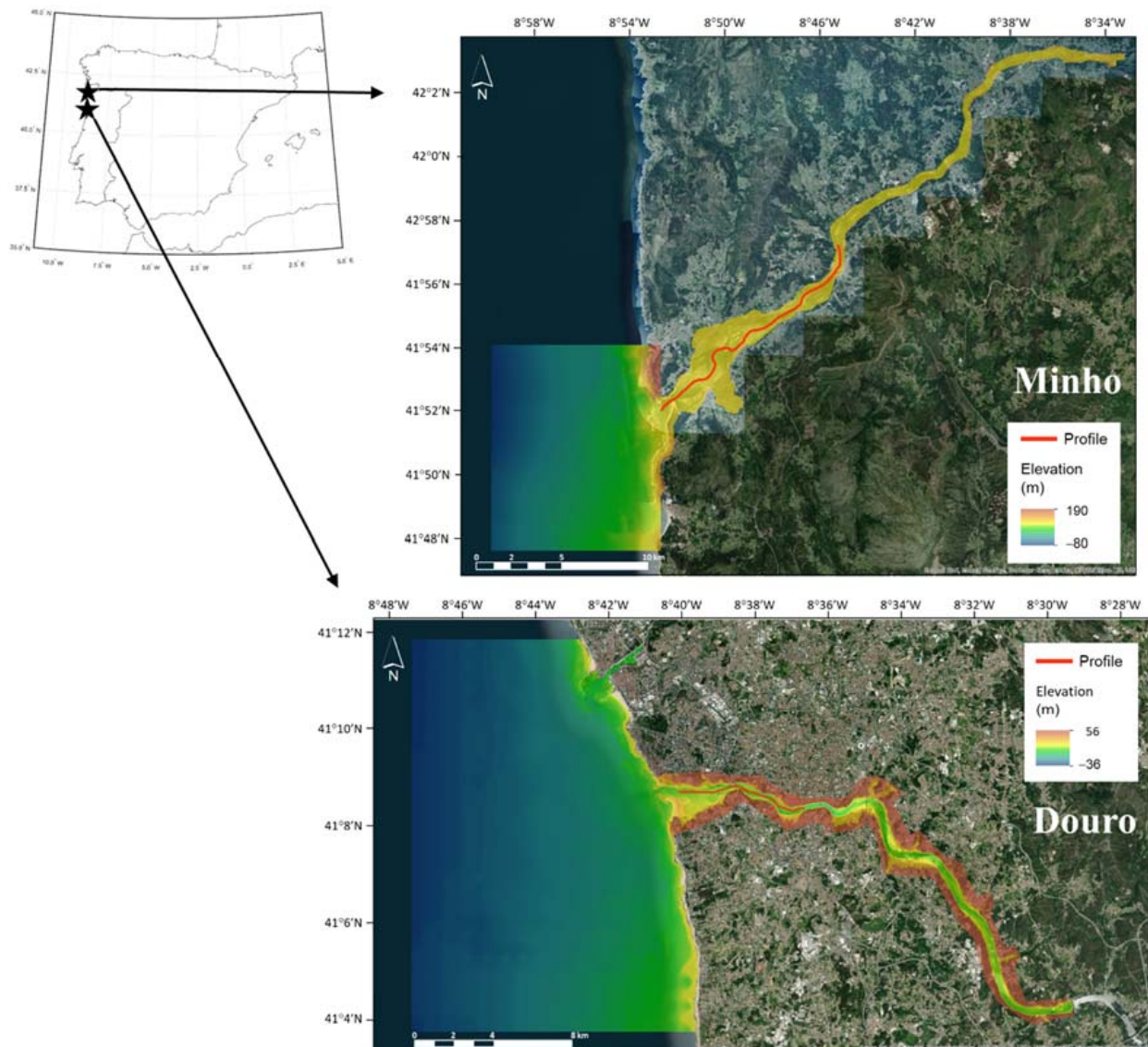


**Figure 1.** Location of the Douro and Minho estuaries, the topo-bathymetries considered for the numerical grids construction and the longitudinal profiles considered for each estuary (base map sources: Esri, Maxar, GeoEye, Earthstar Geographics, CNES/Airbus DS, USDA, USGS, AeroGRID, IGN, and the GIS User Community).

The Minho is an international river that reaches the Atlantic Ocean between La Guardia (Spain) and Caminha (Portugal), constituting a natural border between Spain and Portugal in its last 70 km. The estuary is 40 km long, with sections between 200 m (upriver) and 2000 m wide (near the river mouth). At the mouth, the cross-section is narrower, about 300 m wide [5]. It is a very shallow water body dominated by the tide. Its mean

depth is 4 m, but regions with 11 m or even 20 m depths can be found (Figure 1). The lower estuary presents an accentuated enlargement, which results in a decrease in the currents' velocities, creating favorable conditions for sediment deposition. In fact, one of this estuary's main problems is strong siltation that hampers navigation. Under spring-tide/low-runoff conditions, the Minho estuary effectively imports sediments from the inner shelf [2,21,35]. The estuary presents a semidiurnal, high-mesotidal regime, with a tidal range varying between 2 m and 4 m and an average residence time of 1.5 days associated with low river flows [36]. In this partially mixed system, a vertical stratification can form when a salt wedge structure is generated [37,38]. One of the most important characteristics of the Minho estuarine region is its large diversity of habitats, with several threatened economically and ecologically valuable species, as well as important productivity, which is key for the nursery and feeding of marine species and ecosystem functioning [39,40]. This is the reason why this estuary is protected by Portuguese and Spanish conservation statutes, preserving a low level of urbanization and industrialization [41]. These habitats may be in danger in the current context of climate change due to changes in the salt intrusion. Furthermore, the estuary's strong siltation may exacerbate the impact of future extreme events.

### 3. Materials and Methods

The numerical models selected for this study were the openTELEMAC-MASCARET (OTM) and the Delft3D (D3D). These modeling suites are able to solve similar formulations of the shallow water equations by considering several physical processes, such as tidal forcing, tidal flats, river discharges, the rotation of the Earth, bottom friction, turbulence, sub- and supercritical flows, and water density effects [42–45]. They were also used to simulate hydrodynamic patterns in estuarine areas, assess the flooding risk, and quantify the effects of climate change [46–49]. The models were already calibrated for the selected regions, demonstrating their ability to accurately represent the hydrodynamic characteristics of the Douro and Minho estuaries for both normal and extreme events [5,11,16,21,34]. These models were furthermore selected to demonstrate the feasibility of the ensemble technique, with results showing that an ensemble constructed with weighing techniques reduces the uncertainty of the results and increases the reliability and consistency of predictions for estuarine regions [28].

In the present study, both models were run for several scenarios that considered extreme fluvial discharge (EFD) and extreme sea level (ESL). As described by Robins et al. [8], estuarine flooding can be the volumetric combination of storm surge and extreme river flow. EFD and ESL were considered in the same scenarios because there was evidence of a positive relation between storm surges and peak river flows [50–52]. Several authors suggested that surges should be taken into account for flood risk estimation [53,54].

The EFD for the Douro estuary was calculated using previously published data [55]. Using the parameters of Gumbel's law [56], the relation was rebuilt to calculate the return periods of interest. For the Minho estuary, the EFD was calculated using the values of instantaneous maximum flow in Foz do Mouro, also adapted to Gumbel's law. The river flood peak flows were calculated for 50, 100, and 1000-year return periods.

The ESL values foreseen in the Representative Concentration Pathway scenarios (RCPs) 4.5 and 8.5 for the years 2050 and 2100, for the same return periods considered in the EFD (50, 100, and 1000 years), were extracted from the work of Vousdoukas et al. [57] for the Douro and Minho locations. These authors estimated the total water level conditions along the European coastline from the dynamic simulation of the major hydrodynamic sea level components: mean sea level (MSL), tides, storm surges, and waves. Projections of waves and storm surges were based on hydrodynamic simulations with D3D and WW3 by considering atmospheric forcing from an ensemble of 6 climate models provided by CMIP5 [58]. The database delivers forecasts of average, minimum, and maximum values in agreement with the climate models ensemble results. In the present study, these average, minimum, and maximum forecast values were considered to force the estuarine numerical

models. They give consistency to the estuarine forecasts, providing the average-, best-, and worst-case scenarios, and thus, a range of forecasts. The historical values provided by Vousdoukas et al. [57] were used for comparison with the projections.

A deterministic approach was adopted for this study. Each model that was run consisted of a 24 h long simulation with constant river flow and water elevation boundary conditions, preceded by a spin-up period of 3 h to avoid numerical instabilities. The water elevation modeling results for ensemble construction were extracted at the end of each performed simulation, which was when the models reached a steady state. The numerical modeling scenarios, described in Table 1, were run for both model suites: OTM and D3D.

**Table 1.** Numerical modeling scenarios.

Run	Return Period (Years)	River Flow (m <sup>3</sup> /s)		Scenario	Water Elevation at the Ocean Boundary (m)
		Douro	Minho		
S1	50	17,357	5365	Historical	3.9
S2				RCP 4.5 2050 mean	4.1
S3				RCP 4.5 2050 min	4.0
S4				RCP 4.5 2050 max	4.3
S5				RCP 4.5 2100 mean	4.4
S6				RCP 4.5 2100 min	4.0
S7				RCP 4.5 2100 max	4.8
S8				RCP 8.5 2050 mean	4.2
S9				RCP 8.5 2050 min	3.9
S10				RCP 8.5 2050 max	4.4
S11				RCP 8.5 2100 mean	4.7
S12				RCP 8.5 2100 min	4.2
S13				RCP 8.5 2100 max	5.1
S14	100	19,814	6038	Historical	4.0
S15				RCP 4.5 2050 mean	4.2
S16				RCP 4.5 2050 min	4.1
S17				RCP 4.5 2050 max	4.4
S18				RCP 4.5 2100 mean	4.5
S19				RCP 4.5 2100 min	4.1
S20				RCP 4.5 2100 max	4.9
S21				RCP 8.5 2050 mean	4.2
S22				RCP 8.5 2050 min	4.0
S23				RCP 8.5 2050 max	4.5
S24				RCP 8.5 2100 mean	4.8
S25				RCP 8.5 2100 min	4.3
S26				RCP 8.5 2100 max	5.2
S27	1000	27,962	8262	Historical	4.3
S28				RCP 4.5 2050 mean	4.5
S29				RCP 4.5 2050 min	4.3
S30				RCP 4.5 2050 max	4.7
S31				RCP 4.5 2100 mean	4.8
S32				RCP 4.5 2100 min	4.4
S33				RCP 4.5 2100 max	5.2
S34				RCP 8.5 2050 mean	4.5
S35				RCP 8.5 2050 min	4.2
S36				RCP 8.5 2050 max	4.7
S37				RCP 8.5 2100 mean	5.0
S38				RCP 8.5 2100 min	4.5
S39				RCP 8.5 2100 max	5.4

A superensemble was built for each of the proposed scenarios following the results obtained by Iglesias et al. [28]. For extreme events, the technique that produced the best results in the superensemble construction was the weighted average method that used the squared error as the weight:

$$w_m = \frac{\frac{1}{\mathcal{L}_{SE}}}{\sum_{k=1}^M \frac{1}{\mathcal{L}_{SE|k}}} \quad (1)$$

where  $w_m$  is the weight,  $M$  is the number of simulations that integrate the ensemble, and  $\mathcal{L}_{SE}$  is the squared error metric:

$$\mathcal{L}_{SE} = (X_f - X_o)^2 \quad (2)$$

where  $X_f$  and  $X_o$  are the forecasted and the observed values, respectively, of the variable  $X$ .

Iglesias et al. [28] obtained a weighting coefficient for the observation points of each estuary for the extreme events scenarios. Since we were interested in representing the joint effect of the ESL and EFD on the water levels inside the estuaries, the mean values of these weights were considered for the construction of the superensembles presented here (Table 2).

**Table 2.** Weights considered to construct the superensembles. D1 to D4 (Douro) and M1, M3, and M4 (Minho) were the measurement stations considered to calibrate the ensemble with in situ data (see Iglesias et al. [28] for more information).

Model Suite	Douro					Minho			
	D1	D2	D3	D4	Average	M1	M3	M4	Average
D3D	0.083	0.675	0.640	0.142	0.385	0.829	0.410	0.497	0.579
OTM	0.917	0.325	0.360	0.858	0.615	0.171	0.590	0.503	0.421

Once the ensemble was calculated, results were extracted for a longitudinal profile (Figure 1) to better understand the effect of the river flow and the oceanic elevation, and to represent the effect of the projections in the water level inside the estuaries. Therefore, a longitudinal profile of the free surface water elevation was extracted from the ensemble results for each of the considered estuaries and scenarios (Figures 2 and 3).

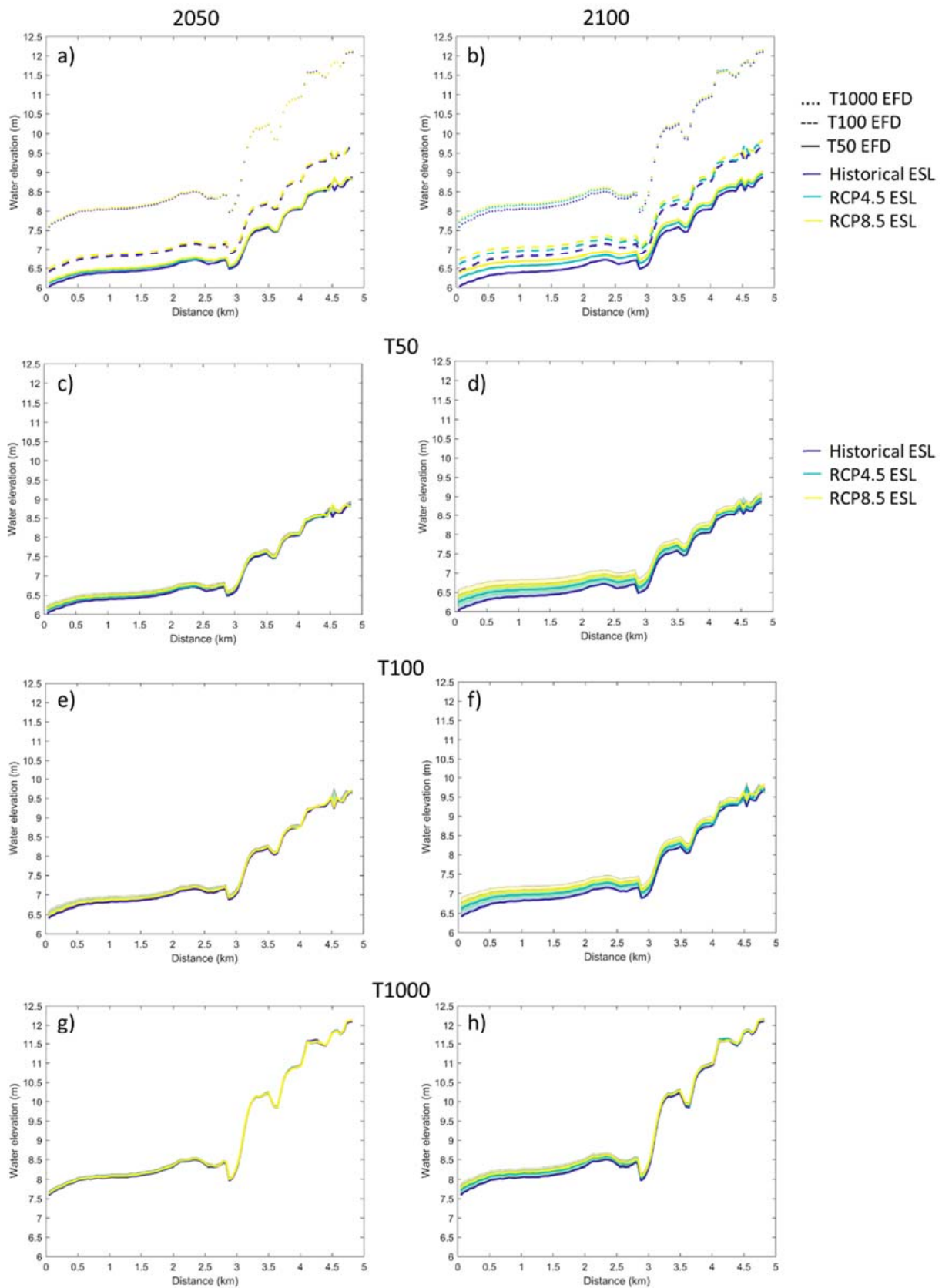


**Figure 2.** Longitudinal profiles of the superensemble solutions that represented the water level along the Douro estuary for the considered scenarios. (a,b) For average values of the water elevations at the ocean boundary; (c–h) Considering the maximum and minimum water elevations values at the ocean boundary to represent the probability forecast.

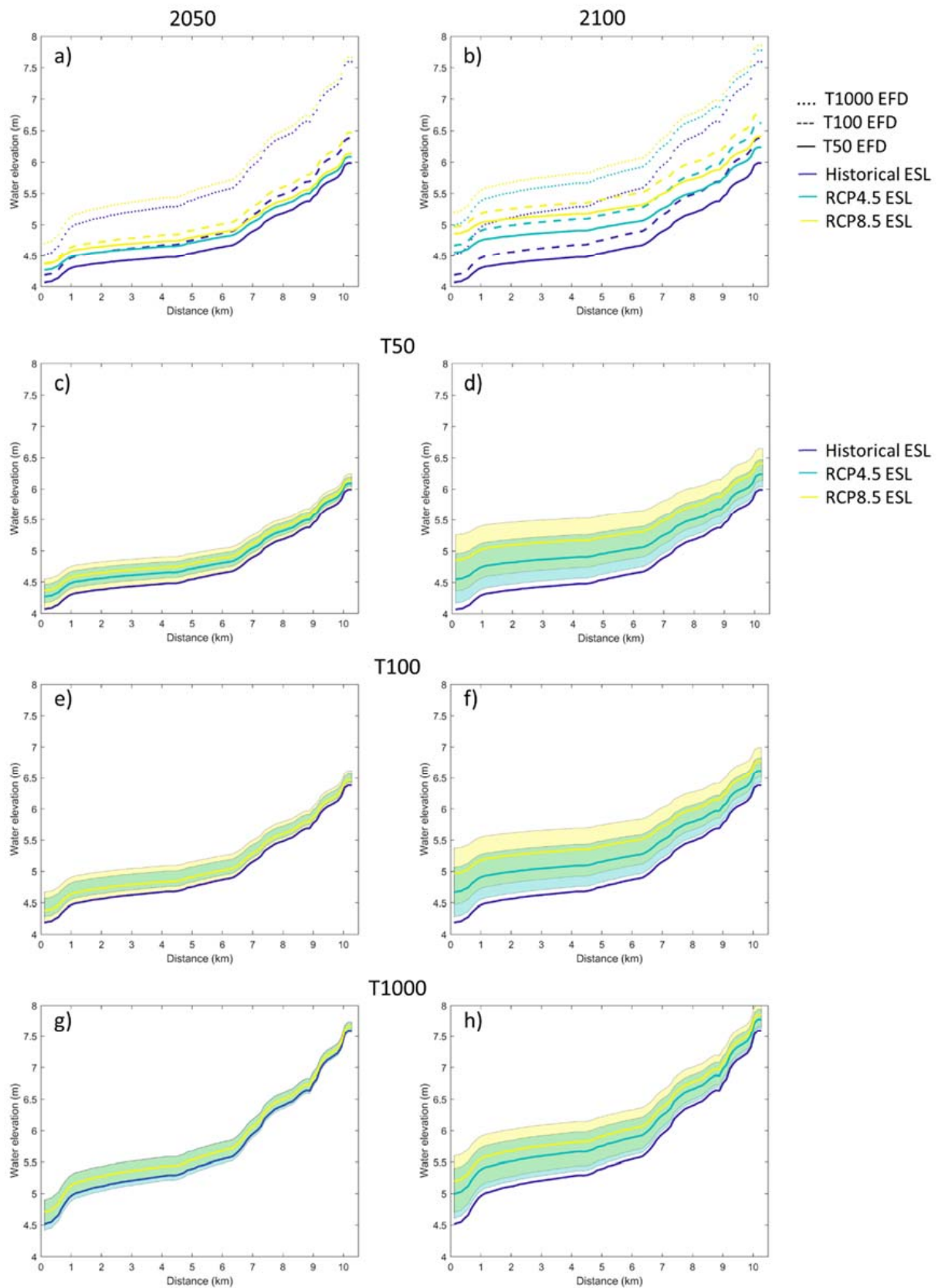


**Figure 3.** Longitudinal profiles of the superensemble solutions that represented the water level along the Minho estuary for the considered scenarios. (a,b) For average values of the water elevations at the ocean boundary; (c–h) Considering the maximum and minimum water elevations values at the ocean boundary to represent the probability forecast.

#### 4. Results

The different water level values predicted by the superensembles for each scenario are presented in Figure 2 for the Douro estuary and in Figure 3 for the Minho estuary. Subfigures a and b from both figures represent the results for 2050 and 2100, respectively, considering only the superensembles constructed with the mean ESL values predicted by Vousdoukas et al. [57] for the historical scenarios (S1, S14, and S27) and the RCP 4.5 (S2, S5, S15, S18, S28, and S31) and 8.5 (S8, S11, S21, S24, S34, and S37) projections. The results showed a clear difference between the hydrodynamic behaviors of the two modeled estuaries.

For the EFD scenarios, the 2050 projections of the water level in the Douro river estuary could reach values between 6 m (at the mouth) and 9 m (5 km upstream) for the 50-year EFD return period, between 6.5 m and 9.7 m for the 100-year return period, and between 7.5 m and 12.2 m for the 1000-year return period (Figure 2a). This meant that between the EFD scenarios for the 50- and 1000-year return periods, water level differences of 1.5 m at the mouth and more than 3 m upstream were observed. The EDF 2100 projections revealed a range of water levels between 6 m and 6.4 m at the mouth and 9 m upstream for the 50-year return period, between 6.4 m and 6.7 m at the mouth and 9.7 m upstream for the 100-year return period, and between 7.5 m and 7.7 m at the mouth and 12.2 m for the 1000-year return period (Figure 2b). For these scenarios, the differences between the 50- and 1000-year return period superensemble results were below 1.7 m at the Douro estuarine mouth and higher than 3 m upstream.

These differences in the water level, jointly with the results of Figure 2a,b, demonstrated that the water elevation in the Douro estuary was weakly dependent on the ESL imposed at the oceanic boundary for flood events, but strongly dependent on the imposed EFD. For 2050, the water level results along the longitudinal profile presented the minimum and the maximum values for the 50- and 1000-year EFD return periods, respectively (Figure 2a). No significant differences were observed to be associated with the ESL forcing values imposed at the oceanic boundary, but it must be noticed that the ESL difference between the historical scenario (S1) and the RCP 8.5 scenarios (S8, S21, and S34) for 2050 was less than 0.3 m. For the 2100 superensemble projections (Figure 2b), slight differences with the imposed ESL became evident inside the Douro estuarine region. However, despite having an ESL forcing that varied over a range of 0.8 m (Table 1), the largest difference in the water level inside the Douro estuary between the S1 historical scenario and the 2100 RCP 8.5 S11 scenario was around 0.4 m. This difference was observed near the mouth, presenting an attenuation upstream and being practically negligible 5 km upstream from the mouth. In addition, the stronger the EFD was, the lower the effect of the ESL inside the Douro estuary, with smaller water level differences for the scenarios that considered the highest ESL (1000-year return period).

For the EFD scenarios, the 2050 superensemble projections of the water level at the Minho river estuary could reach values between 4.0 m and 4.4 m (at the mouth) and around 5.5 m (at 10 km upstream the mouth) for the 50-year EFD return period, between 4.3 m and 6.5 m for the 100-year return period, and between 4.6 m and 7.6 m for the 1000-year return period (Figure 3a). In this estuary, the water level differences were smaller when compared with the Douro estuary, with values between the 50- and 1000-year EFD return periods of 0.6 m at the mouth and of more than 2.0 m upstream. The 2100 superensemble projections revealed a wider range of water level values compared with the Douro estuary, being between 4.0 m and 4.9 m at the mouth and between 6.0 m and 6.5 m upstream for the 50-year EFD return period, between 4.2 m and 5.0 m at the mouth and between 6.5 m and 6.8 m upstream for the 100-year return period, and between 4.5 m and 5.2 m at the mouth and between 7.6 m and 7.9 m upstream for the 1000-year return period (Figure 3b). For the 2100 superensemble projections, water level differences between the 50- and 1000-year return periods were 0.3 m and 0.5 m at the mouth and between 1.4 m and 1.6 m at upstream locations.

The obtained values, jointly with the longitudinal profiles presented in Figure 3a,b, revealed that the water level in the upper Minho estuary was mostly dependent on the imposed EFD, whereas the water level in the lower estuary was mostly dependent on the ESL imposed at the oceanic boundary. The point that separated these distinct behaviors was located around 8.5 km upstream from the river mouth, coincident with the narrowing of the estuarine region. However, contrary to what was observed for the Douro estuary, the sea level rise in the Minho estuary was projected to have an effect along the estuarine region, increasing the water level even at upstream locations. Similar to the Douro estuary, higher differences in the water levels inside the estuarine region between the historical scenarios and the projections were obtained for the superensembles that considered the 2100 projections (Figure 3b). In the Minho estuary, the differences in water level between the scenarios were significant, with values between the historical scenario (S1) and the RCP 8.5 projection for 2100 (S11) reaching 0.8 m near the estuarine mouth.

The superensemble water level projections for the Douro estuary revealed that, for 2050, the minimum and the maximum ESLs forecasted by Vousdoukas et al. [57] did not differ much from the mean simulation results (Figure 2c,e,g). For the 2100 scenarios (Figure 2d,f,h), the difference in the water level between the best and worst projections was more accentuated but still small, with differences around 0.4 m, 0.3 m, and 0.2 m for the scenarios that considered the 50-year, (Figure 2d), 100-year (Figure 2f), and 1000-year (Figure 2h) EFD return periods, respectively. However, these differences were only noticeable in the downstream region of the estuary.

For the Minho estuary, the superensemble projections that considered the minimum and maximum ESLs forecasted by Vousdoukas et al. [57] presented some differences from the projections in the Douro region. First of all, for the 2050 projections (Figure 3c,e,g), a significant difference was found between the water levels obtained for the scenarios that considered maximum and minimum ESLs and the ones that were forced with a mean ESL extracted from Vousdoukas et al. [57]. This difference was around 0.3 m for RCP 4.5 (runs S3 and S4) and around 0.5 m for RCP 8.5 (runs S9 and S10) at the estuarine mouth for the superensemble constructed with the scenarios considering a 50-year EFD return period (Figure 3c). These values were similar to the ones obtained for the scenarios that considered the 100-year (Figure 3e; runs S16, S17, S22, and S23) and the 1000-year EFD return period (Figure 3f; runs S29, S30, S35, and S36). The difference between the RCP projections diminished upstream but was still significant (around 0.3 m) 10 km upstream (Figure 3c,e). An exception was the 1000-year EFD return period (Figure 3g) in which the strong river flow was able to reduce the effect of the ESL at upstream locations. For the 2100 superensembles, differences in water level values between the higher and the lower ESLs imposed were even stronger, with values around 0.8 m for RCP 4.5 (runs S6 and S7) and RCP 8.5 (runs S12 and S13) at the estuarine mouth for the 50-year EFD return period (Figure 3d). Upstream, the difference was around 0.5 m for both projections. Similar values were obtained for the superensemble constructed with the simulations that considered the 100-year return period (Figure 3f), as well as for the projections that considered the 1000-year return period, although only at the estuarine mouth. Upstream, the latter projection presented a difference of less than 0.5 m between the results for the maximum and minimum ESL conditions of each scenario.

In the Douro estuary, for the 2050 and 2100 projections, water levels were expected to reach between 6.0 m and 7.5 m at the estuarine mouth and between 9.0 m and 12.2 m upstream. Meanwhile, for the Minho estuary, depth values were expected to reach between 4.0 m and 4.6 m at the mouth and between 5.5 m to 7.6 m upstream for the 2050 scenario, and between 4.0 m and 4.5 m at the mouth and between 6.5 m and 7.9 m upstream for the 2100 projections. Given the forecasted values, the topographic characteristics of the estuarine banks, and the narrow mouth configuration of both estuaries, strong floods were expected.

The flooded areas according to several superensemble forecastings are presented for the Douro (Figure 4) and Minho estuaries (Figure 5). For the Douro estuary, as demonstrated

in Figure 2, the differences between the scenarios that considered ESLs projected for RCP 4.5 and 8.5 and for 2050 and 2100 were practically negligible. Therefore, only flood maps for the historical scenarios S1, S14, and S27 are presented (Figure 4). For the three historical scenarios, the results suggested that the margins of the Douro estuary will be affected by floods, with more severe damage to be expected near the river mouth and in the valleys of several small affluent rivers at the northern margin. At the southern margin, the floods were projected to affect the sand spit, a marina located near the estuarine mouth, the historical center of Vila Nova de Gaia, and some non-urbanized zones. Other minor areas are also expected to be flooded, affecting roads and buildings next to the estuary margins, but to a lesser extent. Due to the embedded valley configuration of this estuary, the flooding areas are quite restricted; however, water levels of more than 16 m are expected to be reached in the upper part of the studied estuarine area for the 1000-year EFD return period scenario.



**Figure 4.** Water levels in the Douro estuary forecasted for the (a) S1 scenario (historical, 50-year EFD return period), (b) S14 scenario (historical, 100-year EFD return period), and (c) S27 scenario (historical, 1000-year EFD return period) (base map sources: Esri, Maxar, GeoEye, Earthstar Geographics, CNES/Airbus DS, USDA, USGS, AeroGRID, IGN, and the GIS User Community).

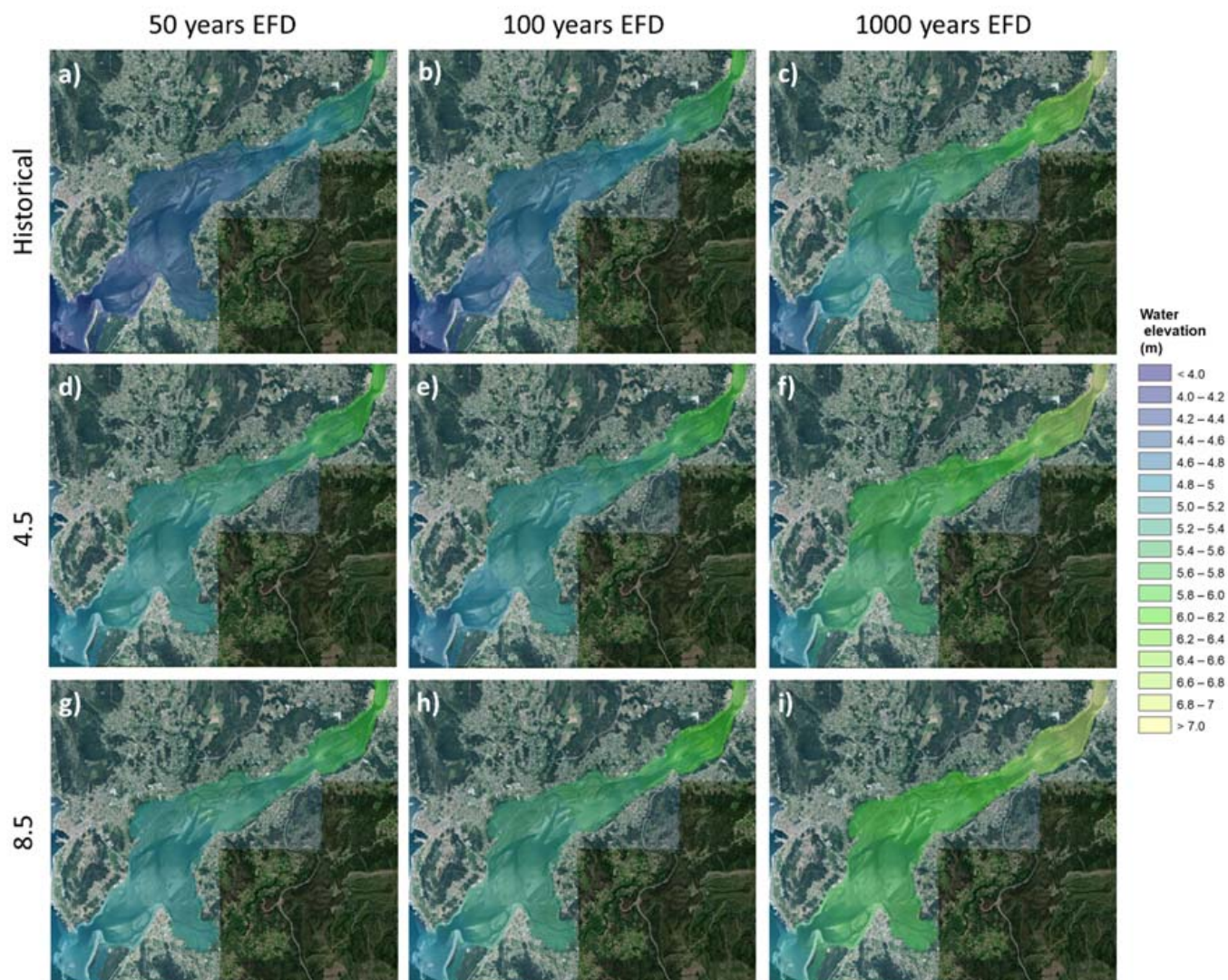


**Figure 5.** Water levels in the Minho estuary forecasted for the (a) S1 scenario (historical, 50-year EFD return period), (b) S14 scenario (historical, 100-year return EFD period), (c) S27 scenario (historical, 1000-year EFD return period), (d) S5 (4.5, 50-year EFD return period), (e) S18 (4.5, 100-year EFD return period), (f) S31 (4.5, 1000-year EFD return period), (g) S11 (8.5, 50-year return EFD period), (h) S24 (8.5, 100-year EFD return period), and (i) S37 (8.5, 1000-year EFD return period) (base map sources: Esri, Maxar, GeoEye, Earthstar Geographics, CNES/Airbus DS, USDA, USGS, AeroGRID, IGN, and the GIS User Community).

In comparison to the Douro estuary, the Minho estuary presented lower water levels, but the predicted flooded areas were larger (Figure 5). Notice that for the simulated scenarios, the flooded areas reached the boundaries of the numerical grids; therefore, harsher effects than the ones presented here can be expected. This is likely to be more relevant at the northern margin because there, the topography varies more smoothly than at the southern margin, which presents sharper topographic transitions, restricting the spreading of the floods. Similar to what can be observed in Figure 3, the highest water levels were obtained upstream and the lowest near the estuarine mouth, coincident with the widening of the estuarine area. There were also marked differences in water level between the scenarios that considered different EFD and ESL values. The obtained water levels were lower for scenario S1 (Figure 5a) and higher for scenario S37 (Figure 5i). Comparing the historical scenarios (Figure 5a–c) with the mean values obtained for RCP 4.5 (Figure 5d–f) and 8.5 (Figure 5g–i), the effects of the ESLs associated with the different sea-level scenarios

became clear. Due to the topographic characteristics of this estuary, the Boega Island (upstream), the sand spit at the estuary mouth, the mouths of the Tamuxe (northern margin) and Coura (southern margin) rivers, and the surroundings of the estuary region were projected to flood according to all of the represented scenarios. However, the forecasted water levels varied with the region, as well as with the considered scenario. The floods are expected to occupy several non-urbanized and agricultural zones (at the northern margin) and small urban environments (at the southern margin), with harsher effects caused by sea-level rise.

## 5. Discussion and Conclusions

In this study, the water level inside two estuarine regions was forecasted by considering several extreme sea level (ESL) scenarios jointly with the occurrence of extreme flood discharge (EFD) events. The scenarios considered EFDs for the Douro and Minho estuaries were calculated for the 50-, 100-, and 1000-year return periods. The ESL values that were foreseen in historical, RCP 4.5 and 8.5 conditions for the years 2050 and 2100 were also selected. These values forced the numerical simulations performed with two high-resolution numerical models, namely, OTM and D3D, which were already calibrated for both estuaries and different scenarios. The obtained results were synthesized in a single solution through the construction of a superensemble for each one of the defined scenarios. In a previous work of the authors, it was demonstrated that this technique improved the accuracy of the forecasting when compared with the individual model results. The constructed superensembles rendered more precise solutions, contributing to a correct characterization of the future hydrodynamics of the studied estuaries, avoiding the errors inherent to each one of the individual models and thus improving the reliability of the presented solutions. To the best of our knowledge, no previous works were devoted to the forecast of future conditions of estuarine hydrodynamics using superensembles.

This work produced important results for local stakeholders and policy makers, with it being innovative in the application of superensembles to predict future scenarios in estuarine regions. Nonetheless, it had some limitations worth mentioning. Given the positive relationship between storm surges and peak river flows found by previous authors, the performed forecastings considered the ESL and EFD conditions jointly. However, extreme events, although important, are not frequent, and the simulations here presented considered forcing conditions for return periods of 50, 100, and 1000 years. Most of the effects of sea-level rise on the biota will likely be produced by changes in the normal hydrodynamic behavior of the estuaries. These changes could only be assessed by considering the effect of sea-level rise on the 3D hydro-morphodynamics conditions, namely, on the salt wedge intrusion, tidal changes, water mixing, and sediment transport. At the same time, the ESL was extracted from a previous work that considered the CMIP5 results for the sea-level rise component. Presently, CMIP6 climate model results are already available, which consider new time frames and new scenarios, and ESL forecasting calculated with CMIP6 is expected to be more accurate, producing, at the same time, more accurate results for the numerical modeling downscaling of estuaries.

It must be stressed that the implemented models are based on the hydrodynamic modules of the OTM and D3D model suites. No sediment transport was considered in the simulations. However, this transport could have a crucial effect on the simulated extreme water levels. If there is a significant sediment transport out of the estuarine region, especially the estuarine sand spits, lower water levels could be expected for both estuaries. Indeed, due to the EFD imposed in the simulations, overtopping and scouring of the estuarine sand spits can be expected, which could at least partially break these structures, augmenting the estuaries' cross-sectional areas and consequently easing water discharge and reducing the water levels upstream. Future studies intend to assess the potential influence of sediment transport and sand spit overtopping on the reduction of flood effects in the Douro and Minho estuarine regions.

Despite the study's limitations, the obtained results revealed marked differences in the hydrodynamic behavior of both estuarine regions, demonstrating how important it is to perform local studies to understand the regional hydrodynamic specificities. Only in this way can detailed and focused information be obtained and provided to the authorities to help them understand the risks and take appropriate measures to reduce the vulnerability of estuarine populations, activities, and environments.

For the Douro estuary, similar results were obtained for the scenarios that considered the same EFD return period. The 2050 projections did not reveal differences with the forcing conditions associated with the ESL values and, even for the 2100 projections, these differences were small and negligible. These results demonstrated that, during an EFD, the ESL effect was attenuated in the Douro River estuary, indicating that the river flow component was more important than the maritime component when flood events were considered. Consequently, no important changes in the hydrodynamic patterns during floods were expected for future scenarios. This river dominance could be explained by the shape and bathymetric configuration of the estuary and its banks, but also by the large hydrographic basin of the Douro River, which produced stronger flood discharges in the estuary compared with other Portuguese rivers. However, and even without the effect of the ESL, the simulated floods obtained for the considered EFD reached several urban regions of the estuary and would likely cause severe economic losses and material damage to its banks. Additional effects on the biota are also expected, as species unable to adapt to drastic changes in salinity will suffer from the increased amount of fresh water, not only in the estuary but also in the adjacent coastal region. Potential effects may be even worse considering that the frequency of extreme events will increase in future projections. The application of appropriate protection and/or mitigation measures for the urban settlements will be essential to reduce vulnerabilities and mitigate the effects of the extreme conditions predicted for future scenarios.

For the Minho estuary, the simulated water level values were smaller than those in the Douro estuary but presented a wider range. Contrary to what was observed for the Douro estuary, the ESL did affect the Minho estuary. This can be explained by the lower flood flows in this basin, but also by the estuarine morphology and the widening of the estuary upstream of the mouth. This widening reduced the water elevation with the EFD. Furthermore, although the entire estuarine region was affected by the ESL, the effect of the ESL was not constant along the entire estuary. The results depended more on the EFD in the upper estuary and more on the ESL in the lower estuary. The point that separated these two regions was located 8.5 km upstream of the river mouth, coincident with the existence of an island (Boega Island) and the narrowing of the estuary. Sea-level rise was projected to produce changes in the estuary's hydrodynamic behavior during floods. Saltier waters are expected in the lower estuary, which can affect the biota of this region, through the expansion of some marine habitats inside the estuary and displacement or even loss of autochthonous ecosystems. In addition, the sedimentation is expected to also be affected, unbalancing morphodynamic patterns and impacting the tidal propagation, with consequences in the entire estuarine region. More marine sediments are expected to enter the estuary and be retained in the lower estuarine region, increasing the siltation problems this estuary is facing. With the whole estuary affected by the ESL, the obtained results revealed differences between the distinct projections, showing a significant worsening of the flood level associated with the EFD and ESL. Nonetheless, damage to urban areas associated with these floods is expected to be lower than those in the Douro estuary due to the lower urbanization level of the Minho estuary. However, given the topography of the estuary, a wider spreading of the floods is expected, which may also negatively affect the unique habitats of this region.

In summary, this work demonstrated the necessity of performing local studies to understand and forecast future hydrodynamic conditions during extreme events in estuarine regions and to delimit flooding areas. Distinct estuarine behaviors were represented, exemplifying different situations that can be extrapolated to other estuaries. At the same

time, the superensembles technique was applied to provide robust forecasts for several RCP scenarios and EFD and ESL conditions, showing how numerical modeling tools can be improved with key information to minimize vulnerabilities and risks in these highly sensitive regions.

**Author Contributions:** Conceptualization: I.I., J.P. and P.A.-V.; methodology: I.I., J.P. and P.A.-V.; computation: I.I., A.B., W.M., P.A.-V. and M.C.; validation: I.I., W.M. and P.A.-V.; formal analysis: I.I., J.P. and P.A.-V.; investigation: I.I.; resources: A.B., J.P., P.A.-V., J.V., L.B. and F.V.-G.; data curation: I.I., A.B., W.M., P.A.-V., M.C. and A.G.; writing—original draft preparation: I.I.; writing—review and editing: A.B., J.P., W.M., P.A.-V., M.C., A.G., J.V., L.B. and F.V.-G.; visualization: I.I., A.B., P.A.-V., and M.C.; supervision: F.V.-G.; project administration: I.I., J.P. and F.V.-G.; funding acquisition: I.I., A.B., J.P., P.A.-V., J.V., L.B. and F.V.-G. All authors have read and agreed to the published version of the manuscript.

**Funding:** This research was partially supported by the Strategic Funding UIDB/04423/2020 and UIDP/04423/2020 through national funds provided by the FCT—Foundation for Science and Technology and European Regional Development Fund (ERDF). This contribution was also funded by the project EsCo-Ensembles (PTDC/ECI-EGC/30877/2017), co-financed by NORTE 2020, Portugal 2020, and the European Union through the ERDF, and by the FCT through national funds.

**Institutional Review Board Statement:** Not applicable.

**Informed Consent Statement:** Not applicable.

**Data Availability Statement:** The raw data supporting the conclusions of this article will be made available by the authors, without undue reservation.

**Acknowledgments:** The authors want to thank project ECOIS—Estuarine Contributions to Inner Shelf dynamics, Direção Geral do Território, Instituto Hidrográfico, Energias de Portugal, and Confederación Hidrográfica Miño-Sil for the data provided.

**Conflicts of Interest:** The authors declare no conflict of interest. The funders had no role in the design of the study; in the collection, analyses, or interpretation of data; in the writing of the manuscript; or in the decision to publish the results.

## References

1. Canuel, E.A.; Cammer, S.S.; McIntosh, H.A.; Pondell, C.R. Climate change impacts on the organic carbon cycle at the land-ocean interface. *Annu. Rev. Earth Planet. Sci.* **2012**, *40*, 685–711. [[CrossRef](#)]
2. Iglesias, I.; Avilez-Valente, P.; Pinho, J.L.; Bio, A.; Vieira, J.M.; Bastos, L.; Veloso-Gomes, F. Numerical Modeling Tools Applied to Estuarine and Coastal Hydrodynamics: A User Perspective. In *Coastal and Marine Environments—Physical Processes and Numerical Modelling*; Antunes do Carmo, J.S., Ed.; IntechOpen: London, UK, 2020; p. 20. [[CrossRef](#)]
3. Dangendorf, S.; Wahl, T.; Hein, H.; Jensen, J.; Mai, S.; Muddersbach, C. Mean Sea Level Variability and Influence of the North Atlantic Oscillation on Long-Term Trends in the German Bight. *Water* **2012**, *4*, 170–195. [[CrossRef](#)]
4. IPCC. Managing the Risks of Extreme Events and Disasters to Advance Climate Change Adaptation. In *Summary for Policymakers*; Cambridge University Press: Cambridge, UK; New York, NY, USA, 2012.
5. Iglesias, I.; Avilez-Valente, P.; Bio, A.; Bastos, L. Modelling the Main Hydrodynamic Patterns in Shallow Water Estuaries: The Minho Case Study. *Water* **2019**, *11*, 1040. [[CrossRef](#)]
6. Dyer, K.R. Response of Estuaries to Climate Change. In *Climate Change: Impact on Coastal Habitation*; Eisma, D., Ed.; CRC Press: Boca Raton, FL, USA, 2021; p. 26. [[CrossRef](#)]
7. Gillanders, B.M.; Elsdon, T.S.; Halliday, I.A.; Jenkins, G.P.; Robins, J.B.; Valesini, F.J. Potential effects of climate change on Australian estuaries and fish utilising estuaries: A review. *Mar. Freshw. Res.* **2011**, *62*, 1115–1131. [[CrossRef](#)]
8. Robins, P.E.; Skov, M.W.; Lewis, M.J.; Giménez, L.; Davies, A.G.; Malham, S.K.; Neill, S.; McDonald, J.E.; Whitton, T.; Jackson, S.E.; et al. Impact of climate change on UK estuaries: A review of past trends and potential projections. *Estuar. Coast. Shelf Sci.* **2016**, *169*, 119–135. [[CrossRef](#)]
9. Vose, R.S.; Applequist, S.; Bourassa, M.A.; Pryor, S.C.; Barthelmie, R.J.; Blanton, B.; Bromirski, P.D.; Brooks, H.E.; DeGaetano, A.T.; Dole, R.M.; et al. Monitoring and Understanding Changes in Extremes: Extratropical Storms, Winds, and Waves. *Bull. Am. Meteorol. Soc.* **2014**, *95*, 377–386. [[CrossRef](#)]
10. Bell, J.E.; Brown, C.L.; Conlon, K.; Herring, S.; Kunkel, K.E.; Lawrimore, J.; Lubert, G.; Schreck, C.; Smith, A.; Uejio, C. Changes in extreme events and the potential impacts on human health. *J. Air Waste Manag. Assoc.* **2018**, *68*, 265–287. [[CrossRef](#)]

11. de Melo, W.W.; Pinho, J.; Iglesias, I.; Bio, A.; Avilez-Valente, P.; Vieira, J.; Bastos, L.; Veloso-Gomes, F. Flood Risk Assessment at the Douro River Estuary. In *Climate Change and Water Security. Lecture Notes in Civil Engineering*; Kolathayar, S., Mondal, A., Chian, S.C., Eds.; Springer: Berlin/Heidelberg, Germany, 2022; pp. 37–49. [[CrossRef](#)]
12. Hallett, C.S.; Hobday, A.J.; Tweedley, J.R.; Thompson, P.A.; McMahon, K.; Valesini, F.J. Observed and predicted impacts of climate change on the estuaries of south-western Australia, a Mediterranean climate region. *Reg. Environ. Chang.* **2018**, *18*, 1357–1373. [[CrossRef](#)]
13. Coelho, C.; Silva, R.; Veloso-Gomes, F.; Taveira-Pinto, F. Potential effects of climate change on northwest Portuguese coastal zones. *ICES J. Mar. Sci.* **2009**, *66*, 1497–1507. [[CrossRef](#)]
14. Bastos, L.; Bio, A.; Iglesias, I. The importance of marine observatories and of RAIAs in particular. *Front. Mar. Sci.* **2016**, *3*, 140. [[CrossRef](#)]
15. Teng, J.; Jakeman, A.J.; Vaze, J.; Croke, B.F.W.; Dutta, D.; Kim, S. Flood inundation modelling: A review of methods, recent advances and uncertainty analysis. *Environ. Model. Softw.* **2017**, *90*, 201–216. [[CrossRef](#)]
16. Iglesias, I.; Venâncio, S.; Pinho, J.L.; Avilez-Valente, P.; Vieira, J. Two Models Solutions for the Douro Estuary: Flood Risk Assessment and Breakwater Effects. *Estuar. Coasts* **2019**, *42*, 348–364. [[CrossRef](#)]
17. Yang, Z.; Wang, T.; Voisin, N.; Copping, A. Estuarine response to river flow and sea-level rise under future climate change and human development. *Estuar. Coast. Shelf Sci.* **2015**, *156*, 19–30. [[CrossRef](#)]
18. Chua, V.P.; Xu, M. Impacts of sea-level rise on estuarine circulation: An idealized estuary and San Francisco Bay. *J. Mar. Syst.* **2014**, *139*, 58–67. [[CrossRef](#)]
19. Vargas, C.I.C.; Vaz, N.; Dias, J.M. An evaluation of climate change effects in estuarine salinity patterns: Application to Ria de Aveiro shallow water system. *Estuar. Coast. Shelf Sci.* **2017**, *189*, 33–45. [[CrossRef](#)]
20. Liu, W.C.; Chan, W.T. Assessment of climate change impacts on water quality in a tidal estuarine system using a three-dimensional model. *Water* **2016**, *8*, 60. [[CrossRef](#)]
21. de Melo, W.W.; Pinho, J.; Iglesias, I.; Bio, A.; Avilez-Valente, P.; Vieira, J.; Bastos, L.; Veloso-Gomes, F. Hydro- and Morphodynamic Impacts of Sea Level Rise: The Minho Estuary Case Study. *J. Mar. Sci. Eng.* **2020**, *8*, 441. [[CrossRef](#)]
22. Cheng, T.K.; Hill, D.F.; Beamer, J.; García-Medina, G. Climate change impacts on wave and surge processes in a Pacific Northwest (USA) estuary. *J. Geophys. Res. Ocean* **2015**, *120*, 182–200. [[CrossRef](#)]
23. Seiffert, R.; Hesser, F. Investigating climate change impacts and adaptation strategies in German estuaries. *Kuste* **2014**, *81*, 551–563.
24. Ahmadian, R.; Olbert, A.I.; Hartnett, M.; Falconer, R.A. Sea level rise in the Severn Estuary and Bristol Channel and impacts of a Severn Barrage. *Comput. Geosci.* **2014**, *66*, 94–105. [[CrossRef](#)]
25. Das, D.M.; Singh, R.; Kumar, A.; Mailapalli, D.R.; Mishra, A.; Chatterjee, C. A Multi-Model Ensemble Approach for Stream Flow Simulation. In *Modelling Methods and Practices in Soil and Water Engineering*; Oakville, O.N., Waretown, N.J., Eds.; Apple Academic Press: New York, NY, USA, 2017; pp. 71–102. [[CrossRef](#)]
26. Suh, M.-S.; Oh, S.-G.; Lee, D.-K.; Cha, D.-H.; Choi, S.-J.; Jin, C.-S.; Hong, S.-Y. Development of New Ensemble Methods Based on the Performance Skills of Regional Climate Models over South Korea. *J. Clim.* **2012**, *25*, 7067–7082. [[CrossRef](#)]
27. Viney, N.R.; Bormann, H.; Breuer, L.; Bronstert, A.; Croke, B.; Frede, H.; Gräff, T.; Hubrechts, L.; Huisman, J.A.; Jakeman, A.; et al. Assessing the impact of land use change on hydrology by ensemble modelling (LUCHEM) II: Ensemble combinations and predictions. *Adv. Water Resour.* **2009**, *32*, 147–158. [[CrossRef](#)]
28. Iglesias, I.; Pinho, J.L.; Avilez-Valente, P.; Melo, W.; Bio, A.; Gomes, A.; Vieira, J.; Bastos, L.; Veloso-Gomes, F. Improving Estuarine Hydrodynamic Forecasts Through Numerical Model Ensembles. *Front. Mar. Sci.* **2022**, *9*, 1–18. [[CrossRef](#)]
29. Tebaldi, C.; Knutti, R. The use of the multi-model ensemble in probabilistic climate projections. *Philos. Trans. R. Soc. A Math. Phys. Eng. Sci.* **2007**, *365*, 2053–2075. [[CrossRef](#)]
30. Re, M.; Valentini, G. Simple ensemble methods are competitive with state-of-the-art data integration methods for gene function prediction. *Proc. Mach. Learn. Res.* **2010**, *8*, 98–111.
31. Bastos, L.; Bio, A.; Pinho, J.L.S.; Granja, H.; Jorge da Silva, A. Dynamics of the Douro estuary sand spit before and after breakwater construction. *Estuar. Coast. Shelf Sci.* **2012**, *109*, 53–69. [[CrossRef](#)]
32. Portela, L. Sediment transport and morphodynamics of the Douro River estuary. *Geo-Mar. Lett.* **2008**, *28*, 77–86. [[CrossRef](#)]
33. Pinto, J.; Silva, A.J. Tide Propagation in the Douro River Estuary (Portugal). In *43rd Estuarine & Coastal Sciences Association—International Symposium*; Faculdade de Ciências da Universidade de Lisboa: Lisboa, Portugal, 2007.
34. Iglesias, I.; Bio, A.; Bastos, L.; Avilez-Valente, P. Estuarine hydrodynamic patterns and hydrokinetic energy production: The Douro estuary case study. *Energy* **2021**, *222*, 119972. [[CrossRef](#)]
35. Santos, A.I.; Oliveira, A.; Pinto, J.P.; Freitas, M.C. Hydrodynamic and Sediment Transport Patterns in the Minho and Douro Estuaries (NW Portugal) Based on ADCP Monitoring Data: Part 1-Tidal Sediment Exchanges. *Coasts* **2021**, *1*, 31–55. [[CrossRef](#)]
36. Ferreira, J.G.; Abreu, P.F.; Bettencourt, A.M.; Bricker, S.B.; Marques, J.C.; Melo, J.J.; Newton, A.; Nobre, A.; Patricio, J.; Rocha, F.; et al. Monitoring Plan for Portuguese Coastal Waters. In *Water Quality and Ecology. Development of Guidelines for the Applications of the European Union Water Framework Directive*; INAG-IMAR: Portugal, 2005; Available online: [https://www.researchgate.net/publication/276921166\\_Monitoring\\_Plan\\_For\\_Water\\_Quality\\_and\\_Ecology\\_for\\_Portuguese\\_Transitional\\_and\\_Coastal\\_Waters\\_Development\\_of\\_guidelines\\_for\\_the\\_application\\_of\\_the\\_European\\_Union\\_Water\\_Framework\\_Directive](https://www.researchgate.net/publication/276921166_Monitoring_Plan_For_Water_Quality_and_Ecology_for_Portuguese_Transitional_and_Coastal_Waters_Development_of_guidelines_for_the_application_of_the_European_Union_Water_Framework_Directive) (accessed on 10 May 2022).

37. Sousa, R.; Guilhermino, L.; Antunes, C. Molluscan fauna in the freshwater tidal area of the River Minho estuary, NW of Iberian Peninsula. *Ann. Limnol. Int. J. Limnol.* **2005**, *41*, 141–147. [[CrossRef](#)]
38. Sousa, M.C.; Vaz, N.; Alvarez, I.; Gomez-Gesteira, M.; Dias, J.M. Modeling the Minho River plume intrusion into the Rias Baixas (NW Iberian Peninsula). *Cont. Shelf Res.* **2014**, *85*, 30–41. [[CrossRef](#)]
39. Domínguez García, M.D.; Horlings, L.; Swagemakers, P.; Simón Fernández, X. Place branding and endogenous rural development. Departure points for developing an inner brand of the River Minho estuary. *Place Brand. Public Dipl.* **2013**, *9*, 124–140. [[CrossRef](#)]
40. Ribeiro, D.C.; Costa, S.; Guilhermino, L. A framework to assess the vulnerability of estuarine systems for use in ecological risk assessment. *Ocean Coast. Manag.* **2016**, *119*, 267–277. [[CrossRef](#)]
41. Freitas, V.; Costa-Dias, S.; Campos, J.; Bio, A.; Santos, P.; Antunes, C. Patterns in abundance and distribution of juvenile flounder, *Platichthys flesus*, in Minho estuary (NW Iberian Peninsula). *Aquat. Ecol.* **2009**, *43*, 1143–1153. [[CrossRef](#)]
42. Jones, E.J.; Davies, A.M. Application of a finite element model to the computation of tides in the Mersey Estuary and Eastern Irish Sea. *Cont. Shelf Res.* **2010**, *30*, 491–514. [[CrossRef](#)]
43. Monteiro, I.O.; Marques, W.C.; Fernandes, E.H.; Gonçalves, R.C.; Möller, O.O. On the Effect of Earth Rotation, River Discharge, Tidal Oscillations, and Wind in the Dynamics of the Patos Lagoon Coastal Plume. *J. Coast. Res.* **2011**, *27*, 120. [[CrossRef](#)]
44. Robins, P.E.; Davies, A.G. Morphological controls in sandy estuaries: The influence of tidal flats and bathymetry on sediment transport. *Ocean Dyn.* **2010**, *60*, 503–517. [[CrossRef](#)]
45. van Maren, D.S.; van Kessel, T.; Cronin, K.; Sittioni, L. The impact of channel deepening and dredging on estuarine sediment concentration. *Cont. Shelf Res.* **2015**, *95*, 1–14. [[CrossRef](#)]
46. Corti, S.; Pennati, V. A 3D hydrodynamic model of river flow in a delta region. *Hydrol. Process* **2000**, *14*, 2301–2309. [[CrossRef](#)]
47. Putra, S.S.; Wegen, M.V.D.; Reyns, J.; Dam, A.V.; Solomatine, D.P.; Roelvink, J.A. Multi Station Calibration of 3D Flexible Mesh Model: A Case Study of the Columbia Estuary. *Procedia Environ. Sci.* **2015**, *28*, 297–306. [[CrossRef](#)]
48. Gomes, M.P.; Pinho, J.L.; Antunes do Carmo, J.S.; Santos, L. Hazard assessment of storm events for The Battery, New York. *Ocean Coast. Manag.* **2015**, *118*, 22–31. [[CrossRef](#)]
49. Horritt, M.S.; Bates, P.D. Evaluation of 1D and 2D numerical models for predicting river flood inundation. *J. Hydrol.* **2002**, *268*, 87–99. [[CrossRef](#)]
50. Samuels, P.G.; Burt, N. A new joint probability appraisal of flood risk. *Proc. Inst. Civ. Eng. Water Marit. Eng.* **2002**, *154*, 109–115. [[CrossRef](#)]
51. Senior, C.A.; Jones, R.G.; Lowe, J.A.; Durman, C.F.; Hudson, D. Predictions of extreme precipitation and sea-level rise under climate change. *Philos. Trans. R. Soc. A Math. Phys. Eng. Sci.* **2002**, *360*, 1301–1311. [[CrossRef](#)] [[PubMed](#)]
52. Svensson, C.; Jones, D.A. Dependence between extreme sea surge, river flow and precipitation in eastern Britain. *Int. J. Climatol.* **2002**, *22*, 1149–1168. [[CrossRef](#)]
53. Keef, C.; Svensson, C.; Tawn, J.A. Spatial dependence in extreme river flows and precipitation for Great Britain. *J. Hydrol.* **2009**, *378*, 240–252. [[CrossRef](#)]
54. Zheng, F.; Westra, S.; Sisson, S.A. Quantifying the dependence between extreme rainfall and storm surge in the coastal zone. *J. Hydrol.* **2013**, *505*, 172–187. [[CrossRef](#)]
55. Plano de Bacia Hidrográfica do Rio Douro. Instituto da Água. 2001. Available online: [https://www.biofund.org.mz/wp-content/uploads/2018/11/1543398280-F1962\\_Relfinal.Pdf](https://www.biofund.org.mz/wp-content/uploads/2018/11/1543398280-F1962_Relfinal.Pdf) (accessed on 10 May 2022).
56. Loaiciga, H.A.; Leipnik, R.B. Analysis of extreme hydrologic events with Gumbel distributions: Marginal and additive cases. *Stoch. Hydrol. Hydraul.* **1999**, *13*, 251–259. [[CrossRef](#)]
57. Vousdoukas, M.I.; Mentaschi, L.; Feyen, L.; Voukouvalas, E. Earth’s Future Extreme sea levels on the rise along Europe’s coasts. *Earth’s Future* **2017**, *5*, 304–323. [[CrossRef](#)]
58. Hurrell, J.; Visbeck, M.; Pirani, P. WCRP Coupled Model Intercomparison Project—Phase 5-CMIP5. *Clivar Exch.* **2011**, *16*, 1–32.